Supporting Information

Freely-shapable fabrication of aerogel patterns and 3D architectures by freeze-assisted transfer printing

Wenbo Li[ab], Jing Liu[b], Danyang Liu[a], Jing Li[ab], Jiawei Wang[b], Jiongli Li[b], Xudong Wang[b]*, Meng Su[c]*, Chunbao Li[d]*, and Yanlin Song[c]

[a.] *AECC Beijing Institute of Aeronautical Materials, Beijing Engineering Research Centre of Graphene Application, Beijing 100095, P. R. China*

[b.] *Beijing Institute of Graphene Technology, Beijing 100094, P. R. China. E-mail: netfacn@163.com*

[c.] *Key Laboratory of Green Printing, Institute of Chemistry, Chinese Academy of Sciences (ICCAS), Beijing Engineering Research Center of Nanomaterials for Green Printing Technology, Beijing National Laboratory for Molecular Sciences (BNLMS), Beijing 100190, P. R. China. E-mail: sumeng1988@iccas.ac.cn*

[d.] *Peoples Liberat Army Gen Hosp, Med Ctr 4, Dept Orthopaed Med, Beijing, 100853, P. R. China. E-mail: cli301@foxmail.com*

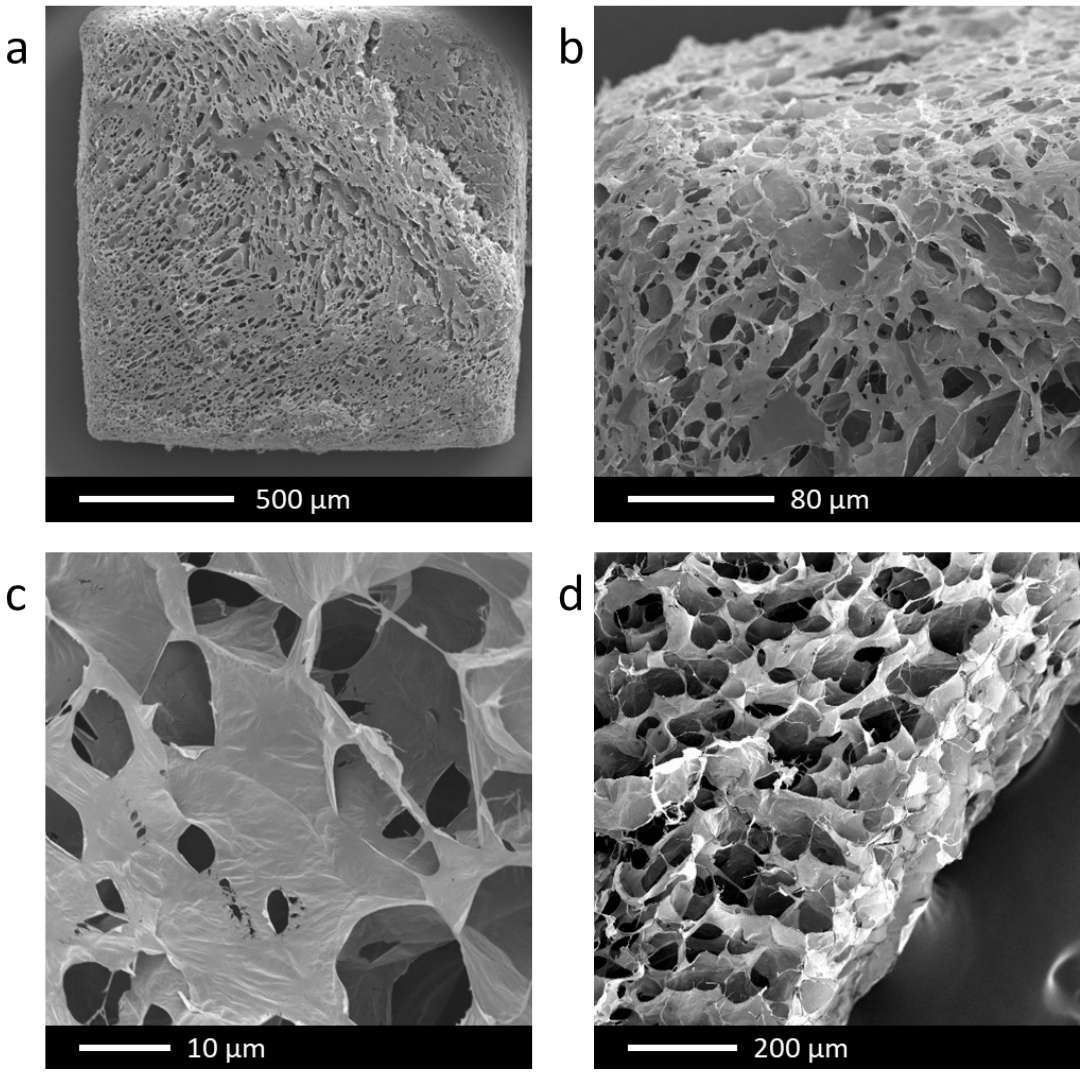

Fig. S1 The typical microscopic morphology of the cubic shaped (a-c) and the linear shaped (d) aerogels units.

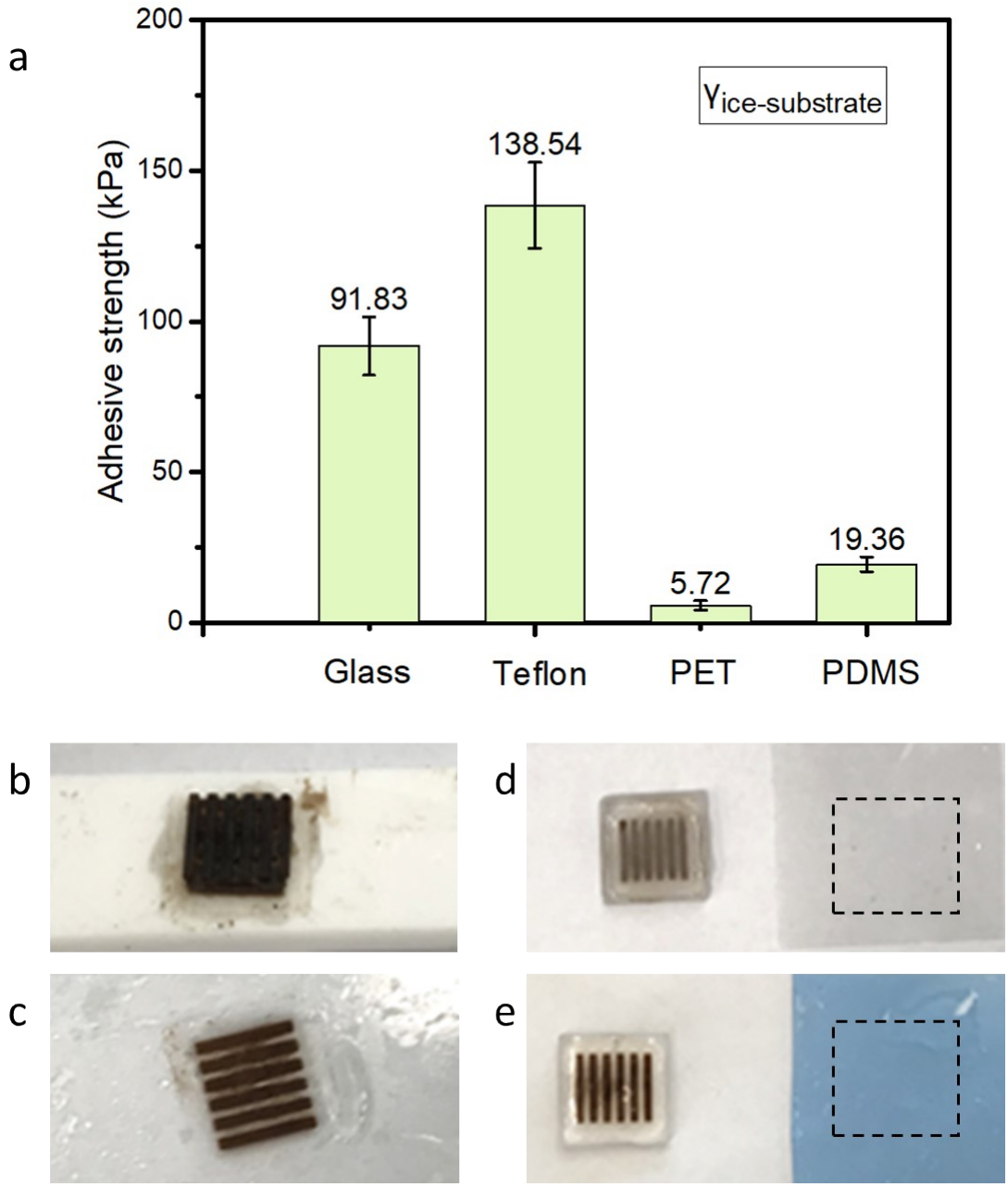

Fig. S2 (a) A comparative analysis on the adhesive strength among the four types of printing substrates. Photographs showing the frozen ices were successfully transfer printed on (b) Teflon and (c) glass substrates, while failed to complete the transfer printing process on (c) PET and (d) PDMS substrates.

The test results show that Teflon can also be used as substrate to complete transfer printing, but the glass substrate is relatively more conventional and easier to obtain, with a lower cost, so glass is adopted in this experiment. While the PET and PDMS are unable to complete the transfer printing process, because they behave lower or equal values of adhesion strength to ice layer than $\gamma_{ice\text{-}stamp}$.

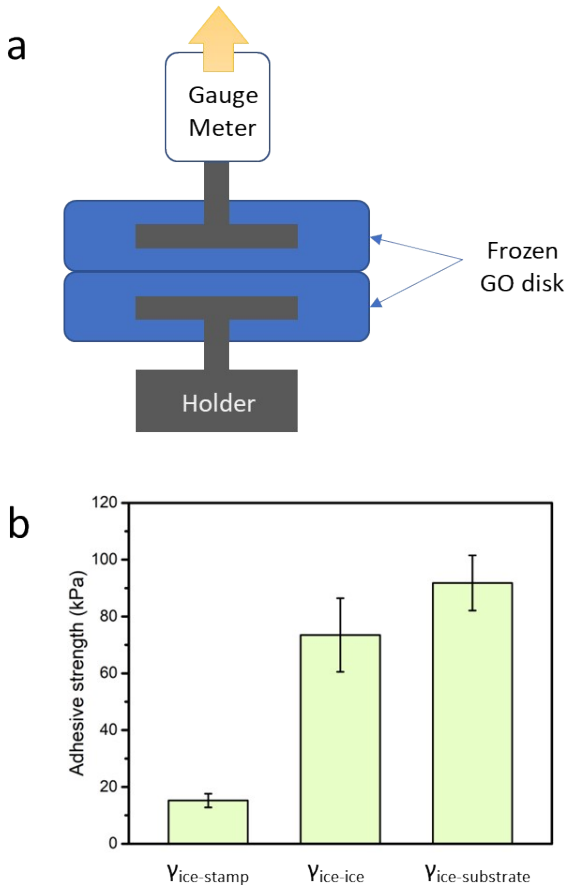

Fig. S3 (a) Two samples of frozen GO disk (with diameter of 15mm and thickness of 1.5mm) were attached together to measure the value of $\gamma_{ice\text{-}ice}$. One of the samples was fixed with a holder, and the other one was connected with a gauge meter. (b) A comparative analysis on the adhesive strength among the three interfaces. The value of $\gamma_{ice\text{-}ice}$ is higher than $\gamma_{ice\text{-}stamp}$, and approximate to $\gamma_{ice\text{-}substrate}$. Thus, the subsequent layers can be transferred to previous layers, similar to that be transferred to glass substrate.

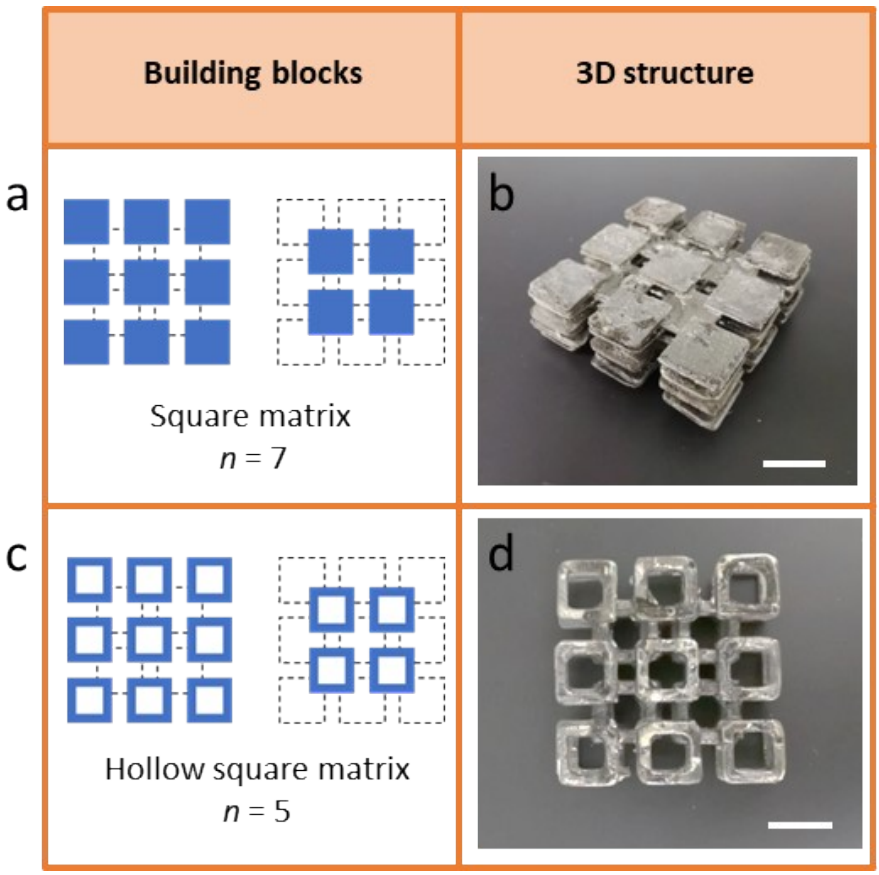

Fig. S4 Additional examples of complex aerogel architectures by FATP. (a, b) The square matrix was staggered arrangement with 3 × 3 and 2 ×2 arrays, with the repeating layers of 7. (c, d) Hollow square shaped building blocks were assembled, with the repeating layers of 5. The scale bars in the figures are 1 cm.

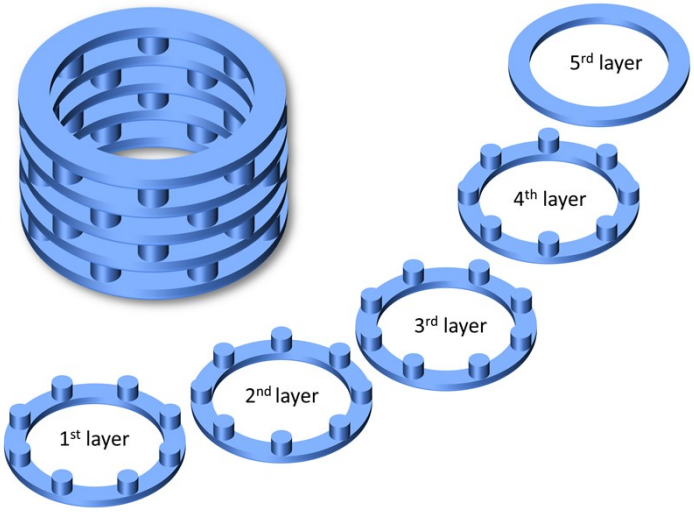

Fig. S5 The structure was prepared with two types of building blocks by five layer of transfer printing. Non-planar patterns that containing torus with pillars were directly printed as layer 1-4. A torus was finally printed as layer 5. These layers are bonded with the pillars.

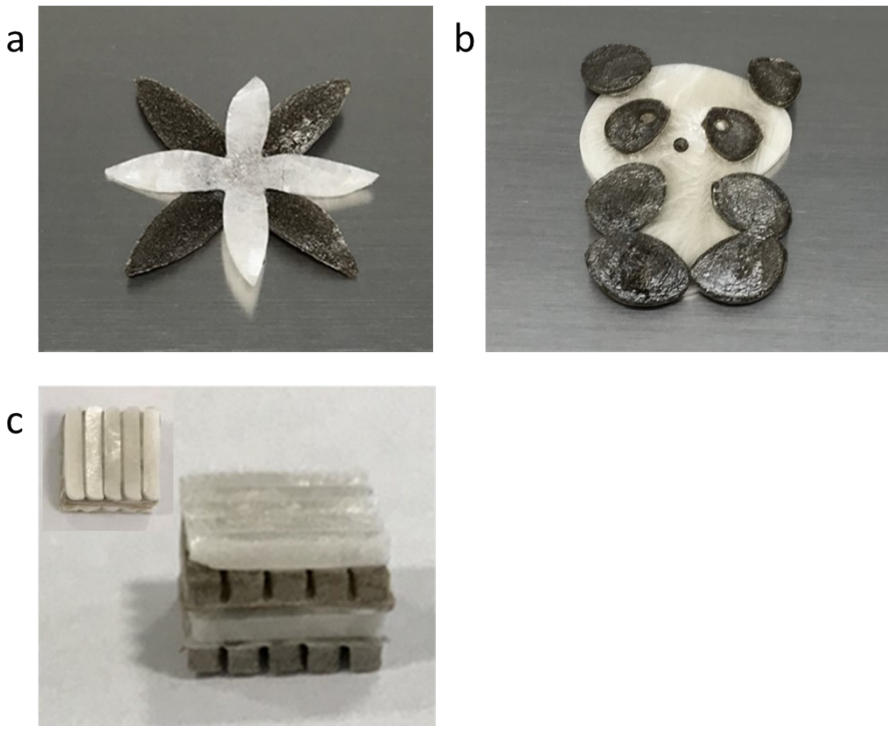

Fig. S6 Heterogeneous aerogel structures showing the ability of FATP for multi materials integration. The designed patterns of (a) petal, (b) panda and (c) woodpiles were fabricated.

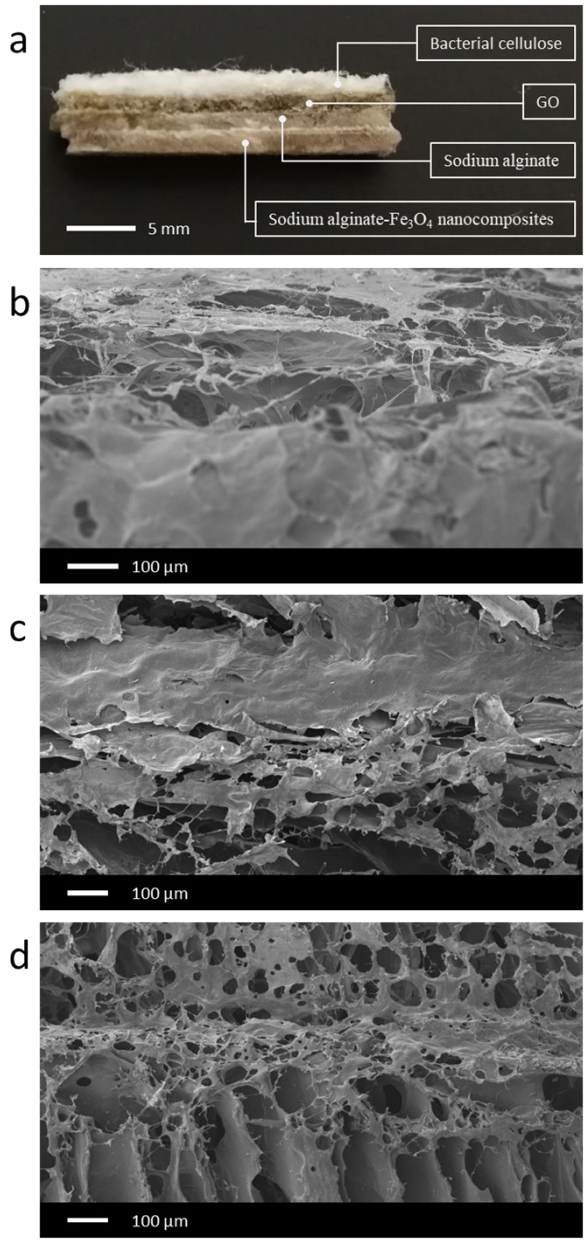

Fig. S7 (a) Heterogeneous integrated aerogel by stacking sequence of sodium alginate-Fe_3O_4 nanocomposites, pure sodium alginate, GO and bacterial cellulose. Three groups of heterogeneous interfaces were formed and their morphology are presented. (b) Interfacial morphology of bacterial cellulose / GO. (c) Interfacial morphology of GO / sodium alginate. (d) Interfacial morphology of sodium alginate / sodium alginate-Fe_3O_4 nanocomposites.

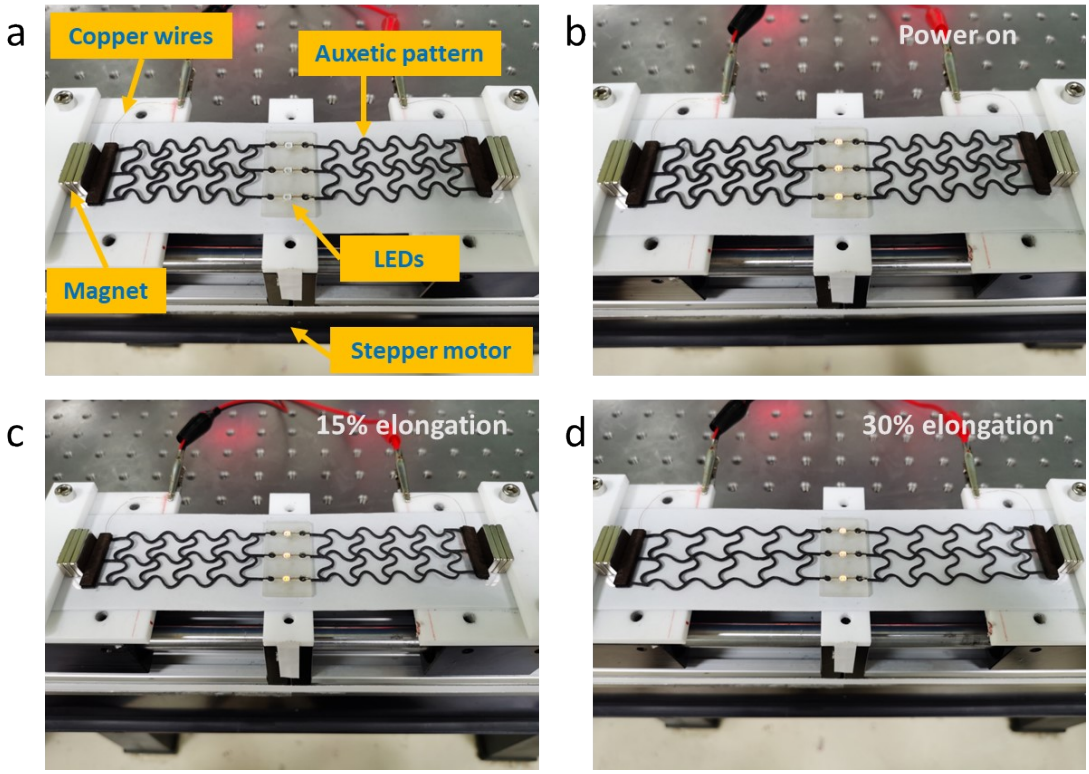

Fig. S8 (a) Detailed construction for the stretchable device. (b)Power on to light the LEDs in the initial state. (c, d) The LEDs maintained consistent brightness strain range of 15% or 30%.